DOI https: //doi. org/10.1007/s11595-018-1922-9

Mechanical Behavior of Polyurethane Polymer Materials under Triaxial Cyclic Loading: A Particle Flow Code Approach

LIU Heng[1,2], WANG Fuming[1], SHI Mingsheng[1*], TIAN Wenling[3]

(1. School of Water Conservancy and Environment, Zhengzhou University, Zhengzhou 450001, China; 2. School of Civil and Transportation Engineering, Henan University of Urban Construction, Pingdingshan 462000, China; 3. State Key Laboratory for Geomechanics and Deep Underground Engineering, China University of Mining& Technology, Xuzhou 221116, China)

Abstract: Polyurethane polymer grouting materials were studied with conventional triaxial tests via the particle flow code in two dimensions (PFC^{2D}) method, and the simulation results agreed with the experimental data. The particle flow code method can simulate the mechanical properties of the polymer. The triaxial cyclic loading tests of the polymer material under different confining pressures were carried out via PFC^{2D} to analyze its mechanical performance. The PFC^{2D} simulation results show that the value of the elastic modulus of the polymer decreases slowly at first and fluctuated within a narrow range near the value of the peak strength; the cumulative plastic strain increases slowly at first and then increases rapidly; the peak strength and elastic modulus of polymer increase with the confining pressure; the PFC^{2D} method can be used to quantitatively evaluate the damage behavior of the polymer material and estimate the fatigue life of the materials under fatigue load based on the number and the location of micro-cracks. Thus, the PFC^{2D} method is an effective tool to study polymers.

Key words: polymer; particle flow code; cyclic loading; elastic modulus; micro-cracks; axial strain

1 Introduction

Non-water reacted polymer grouting materials produced via a two-component polyurethane foam are a new kind of grouting materials[1]. The polymer has excellent comprehensive performance including good chemical stability, high expansion force, high compression strength, long-term durability[2], low permeability, non- environmental pollution, etc. Floors can be lifted by injecting the two-component polyurethane polymer material at predetermined points and using the volume of rapid expansion and solidification after the chemical reaction to fill the voids. Polymer materials have been widely used in the field of foundation reinforcement[3], tunnel leakage stoppage, geotechnical anchorage[5], dam reinforcement to stop seepage, *etc*[4,6].

Despite the widespread use of polymer materials, there are few published studies on the polymers under complex stress. Laboratory tests have focused on the material response under a single stress path such as uniaxial compression[7], uniaxial tension, flexure, etc. Meanwhile, theoretical research on similar polyurethane polymers has mainly used a microscopic model of the 'cell body' to predict the strength with different densities of polymer materials[8,9]. The response could not be predicted when the material was under stress. Numerical calculations of a polymer material are mainly based on finite element methods[10,11]; However, the finite element is dependent on constitutive equations. This can lead to a constitutive relationship that has a significant impact on the numerical testing results.

The scanning electron microscopic (SEM) data in Fig.1 show that the polymer consists of a series of cell bodies with different diameters. In accordance with the PFC method, these materials are an assembly composed of arbitrary spherical particles (in the 3D case) or circular disks (in the 2D case) in the PFC program[12]. Therefore, the PFC can be used to study the mechanical behavior of the polymer material.

Here, conventional triaxial experiments were first performed to calibrate the intact polymer micro-mechanical parameters. Based on the experimental results of polymer specimens under conventional triaxial compression, a set of micro-parameters in PFC^{2D} reflecting the macroscopic mechanical behavior of polymer samples were obtained. The cyclic loading

(Received: May 30, 2017; Accepted: Aug. 10, 2017)

LIU Heng(刘恒): Ph D: Email:yunzhong98@126.com

*Corresponding author: SHI Mingsheng(石明生): Prof.; Ph D; E-mail: sms315@126.com

Funded by the National Key R&D Program of China (No. 2017YFC0405002)

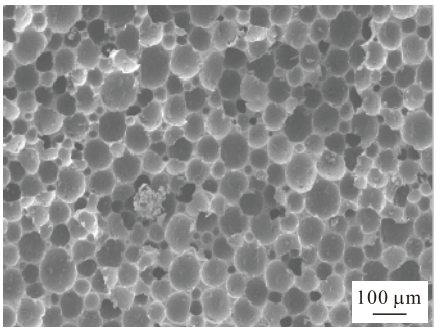

Fig. 1 SEM image of a polymer material (0.35 g/cm^3)

numerical experiments of polymer samples under different confining pressures in the PFC^{2D} were carried out to analyze the elastic modulus, plastic strain, and the evolution of micro-cracks. PFC^{2D} is an innovative method for the research on the mechanical behavior and failure mechanisms in polymers.

2 Experimental

2.1 Preparation

There were 3 polymer specimens in this experiment. The specimens were shaped into cylinders with a diameter of 50 mm, a length of 100 mm, and a density of 0.35 g/cm^3. Both ends of each specimen were polished for loading.

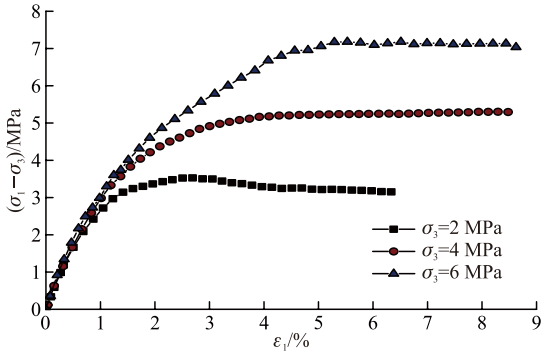

Fig.2 Stress-strain curves of polymer specimens under different confining pressures

An electrohydraulic servo rock triaxial test machine (TAW-2000) was used for the conventional triaxial compression tests. Three confining pressures (2, 4, and 6 MPa) were used to investigate the effect of the confining pressure on the polymer specimen deformation and failure. Here, the ambient temperature was 20 ℃. In a conventional triaxial test, σ_3 is the confining pressure, $(\sigma_1-\sigma_3)$ is the deviatoric stress, and ε_1 is the axial strain.

2.2 Experimental results

Fig.2 shows the stress-strain curves of the specimens for different confining pressures. The stress increases with axial strain, and a greater confining pressure results in a higher peak strength. The curves also indicate that the polymer is an elastic-plastic material, and its performance under a triaxial stress state can be divided into 'two stages.' The first stage is an elastic stage, and the curves are nearly linear; However, the polymer begins to yield at the end of this stage. The second stage results in a hardening stage. The stress increases with increasing strain and tends to be constant; However, the stress-hardening phenomenon is more obvious when the polymer sample is under a higher confining pressure.

3 Simulation

3.1 Brief introduction to PFC^{2D}

The PFC^{2D} is a discrete element method (DEM) for numerical simulation, which is used to model physical problems that are concerned with the movement and interaction of circular particles. It is efficient and has been widely used for geo-materials (soils, rocks, and granular materials)[13,14]. The PFC sample is composed of bonded rigid particles that interact only at contacts or interfaces between particles. Newton's second law is integrated for each particle and provides the updated velocities and new positions. This gives a set of contact forces that act on the particle. This method is effective because it does not require the formulation of complex constitutive models.

Table 1 Micro-parameters in PFC^{2D}

Micro-parameters	Value
Minimum ball radius /mm	0.275
R_{max}/R_{min}	2.7
Ball-ball contact modulus /Pa	3.85×10^8
Ball stiffness ratio, k_n/k_s	1.7
Ball friction coefficient	0.15
Locked-in isotropic stress/Pa	9×10^4
Contact-bond normal strength /Pa	2.12×10^6
Contact-bond normal strength std. dev/Pa	4.3×10^5
Contact-bond shear strength /Pa	2.12×10^6
Contact-bond shear strength std. dev /Pa	4.3×10^5

There are two walls in the PFC^{2D} program-finite walls and infinite walls. The walls are used to apply boundary conditions or as loading platen. There are also two kinds of particle bonding behavior-parallel bonds and contact bonds. Both of these can be envisioned as a kind of glue that joins the two neighboring particles.

The contact bond model was adopted here to

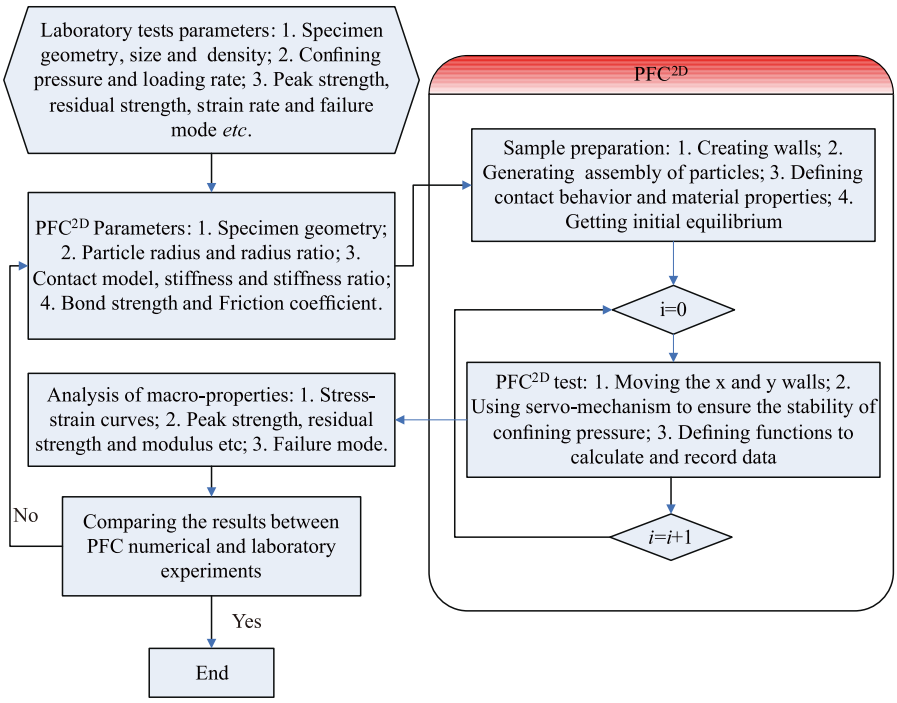

Fig.3 PFC^{2D} micro-parameters calibration process

simulate the contacts between the particles using the PFC^{2D} micro-parameters listed in Table 1. The micro-parameters are related to the macro parameters of the intact material. One of the requirements for PFC^{2D} is the calibration of the micro-contact parameters to match the macro-scale response. Only validated numerical models and micro-parameters can be used to study the polymer materials under other conditions.

3.2 Methodology

Fig.3 shows the general methodology of the PFC^{2D} micro-parameter calibration process. Here, the PFC^{2D} simulation results were compared to the laboratory experimental data. The goal was to verify or calibrate the numerical models.

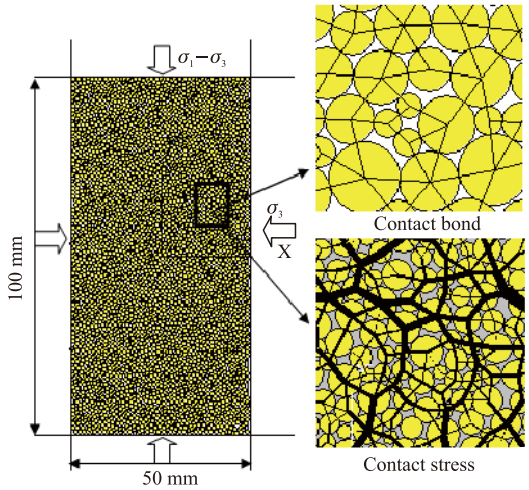

Fig.4 PFC^{2D} model of polymer sample

3.3 The PFC^{2D} model of polymer

The polymer material in PFC^{2D} is an assembly of circular particles (Fig.4). There are four walls, and the top and bottom walls simulate loading platens and provide deviatoric stress[15]. The left and right walls simulate the confinement and provide a confining pressure. Through a trial and error procedure, the micro-parameters in PFC^{2D} were obtained (Table 1).

3.4 Loading method

The sample is loaded in a strain-controlled fashion by specifying the velocities of the top and bottom walls. During all stages of the test, the velocities of the left and right walls were controlled automatically by a numerical servo-mechanism that maintained a constant confining pressure within the sample. Here, monotonic loading and cyclic loading tests were simulated respectively with confining pressures of 2, 4, and 6 MPa.

The cyclic loading experiments consisted of the following steps: the confining pressure was first applied, and then deviatoric stress was loaded onto the surface of the specimen until the axial strain reached the desired value[16]. The platen (top and bottom walls) directions were reversed to unload the specimen until the deviatoric stress ($\sigma_1-\sigma_3$) was reduced to 0.1 MPa. The preceding steps were repeated until the desired strain level was achieved. During the testing, the material response was computed by tracking the various stress and strain quantities using history logic in PFC^{2D}.

4 Results and discussion

4.1 PFC^{2D} micro-parameters validation

The stress-strain curves of polymer from the laboratory tests and PFC^{2D} simulation under different confining pressure are shown in Fig.5. The stress-strain curves, the peak stress of both laboratory tests, and PFC^{2D} simulations show perfect agreements under different confining pressures. For additional verification, Fig.6 shows the failure modes in PFC^{2D} as well as laboratory tests. Here, the distribution of micro-cracks in the numerical sample is very scattered, and there is no shear zone. Greater confining pressures caused more scattering in the micro-cracks. The failure mode in both laboratory and PFC^{2D} tests is axial compression failure-the axial strain increased without any increased stress. The simulation can explain the 'two stages' of the stress-strain curves mentioned in Section 2.2. In the first stage, the initial stress is small, and the bond between the particles does not break. Deformation of the specimen is nearly linear and elastic. During the second stage, some bonds break with the increased load. The particle displacement makes the sample more compact. In the meantime, a cumulative plastic strain has occurred.

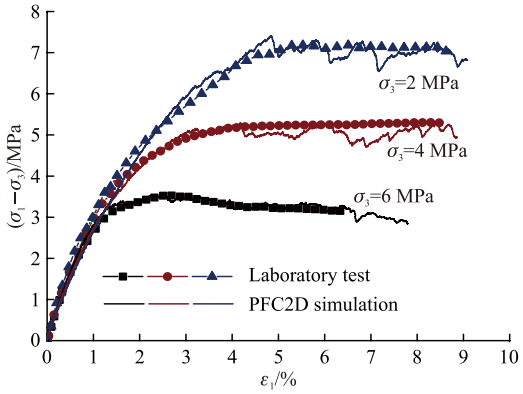

Fig.5 Comparison of stress-strain curves from laboratory tests as well as PFC^{2D} simulation data from different confining pressures

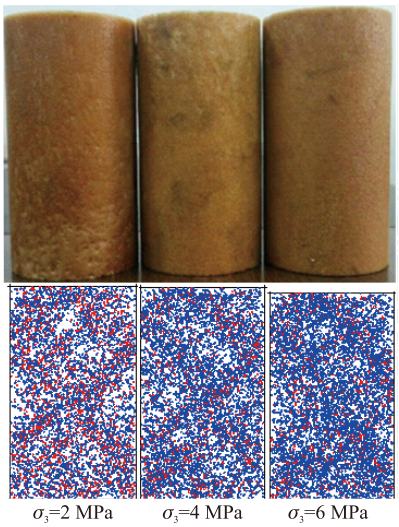

Fig.6 Sample failure in a triaxial test for the calibrated PFC^{2D} micro-parameters as well as observed failure

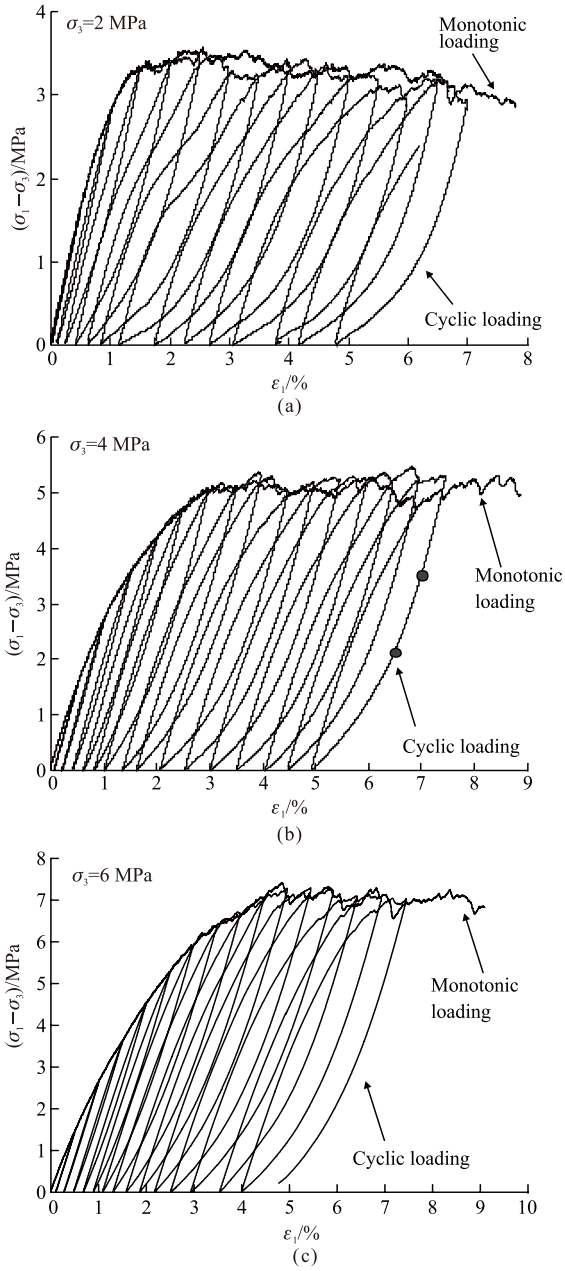

Fig.7 Stress-strain curves of samples under monotonic loading and cyclic loading

The PFC^{2D} data was validated with laboratory tests. The PFC^{2D} contact bond model can simulate the mechanical behavior of the polymer material and the response of the polymer under microscopic loading. Moreover, the PFC^{2D} numerical simulations are better than experimental tests due to the limits of equipment capacity and experimental conditions[17].

4.2 Macro-response of polymer under triaxial cyclic loading

Fig.7 presents the stress-strain curves of samples under a monotonic loading and cyclic loading. Even if the confining pressure is different, the strength envelope of each curve under cyclic loading is similar to the stress-strain curve of monotonic loading. Moreover, the plastic strain increases gradually over a single cycle with increasing load cycles.

4.3 Elastic modulus evolution

Fig.8 shows the elastic modulus of the sample evolution with axial strain under different confining pressures. The elastic modulus first decreases slightly until the axial strain is close to 4%. It then fluctuates within a narrow range. For σ_3=2 MPa, the phenomenon is more obvious. From macroscopic analysis, the structure of the polymer is prone to be disturbed or damaged under cyclic loading. This decreases the elastic modulus. After the peak load, the plastic deformation is bigger, and the porosity decrease increases the elastic modulus slightly and provisionally. During the unloading process, the porosity increases slightly, and the elastic modulus decreases again. On the micro scale of the PFC^{2D} model, the contact force distribution is not uniform. The bonds of some particles break because the contact force is greater than the contact bond strength. This decreases the elastic modulus. Although the bond breaks, the contact force is still changing with cyclic loading. This makes the particles slide or rotate, and friction changes with the contact force. The result is an elastic modulus that fluctuates within a narrow range.

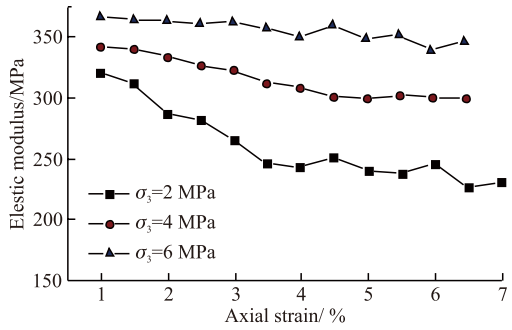

Fig.8 Elastic modulus of samples versus axial strain under different confining pressures

Fig.8 shows that a larger confining pressure results in an elastic modulus with a greater corresponding strain. The confining pressure is beneficial and improves the strength of the polymer material.

4.4 Cumulative plastic strain

The deformation of materials is divided into recoverable elastic deformation and irreversible plastic deformation. The cumulative plastic strain can be used to depict the damage of the materials[18]. Fig.9 shows the cumulative plastic strain evolution with an axial strain under different confining pressures. This shows that before the axial strain reaches 3.5%, the plastic strain increases slowly. A greater confining pressure causes higher plastic strain. After the axial strain increases beyond 3.5%, the plastic strain increases rapidly. A greater confining pressure slows the plastic strain growth and the peak cumulative plastic strain.

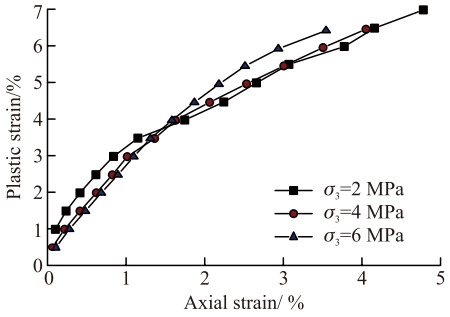

Fig.9 Cumulative plastic strain versus axial strain under different confining pressures

The above phenomenon is because at the beginning of the test, the polymer sample was kept in an elastic state with a small plastic strain. After the peak stress, the sample came into a yield situation, and the plastic strain increased rapidly. Greater confining pressures lowered the accumulated plastic strain. The confining pressure was beneficial to restraining the plastic deformation and improving the resistance to polymeric deformation.

4.5 Micro-cracks evolution

Sample damage is due to the generation, propagation and coalescence of micro-cracks. The PFC^{2D} can record the location and number of micro-cracks during the test. This quantitatively analyzes the internal damage of the polymers and provides a basis for the study of the mechanism of material damage.

Fig.10 shows the total number of micro-cracks in the sample with changes in axial strain during monotonic loading and cyclic loading at a confining pressure of 4 MPa. Under this cyclic loading condition, the number of micro-cracks increased stepwise. At the end of the test, the total number of micro-cracks was 9.65% higher than a monotonically loaded sample. The number of micro-cracks increased slowly during the earlier and later periods with both monotonic and cyclic loading, but this increased rapidly near the peak stress. This is because the bond strength of the particles

is bigger than the contact force in the area of stress concentration during initial loading. The bonds of some particles break and a few cracks are generated. Then, the contact force increases as the load increases, and this quickly generates micro-cracks. Subsequently, some particles are shifted in the sample, and the new cracks are mainly caused by friction or extrusion on the surface of the original cracks. However, the number of new micro-cracks is less, and the position is relatively concentrated. Therefore, at the end of the test, the number of micro-cracks has increased slowly.

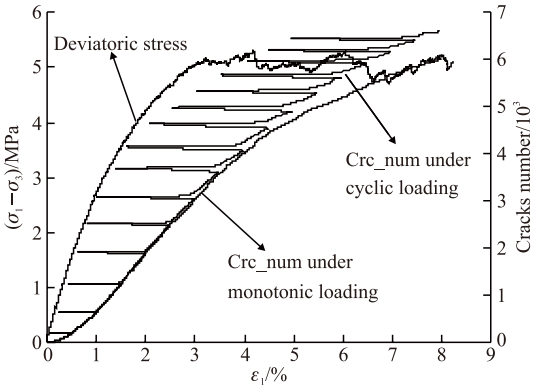

Fig.10 Total number of micro-cracks (crc_num) versus axial strain (σ_3=4MPa)

Fig.10 also shows that under the effect of the first three levels of cyclic loading, the number of micro cracks was the same as that under monotonic loading. It remained unchanged and had "good-memory"[19] after three rounds of loading/unloading strain. During the fourth cycle, the number of cracks began to increase before the axial strain reached the original unloading strain. This is "non-memory" even if the increase is not significant. At this point, the stress was about 40% of the peak stress. During the eighth cycle, the stress reached a peak value, and the numbers of cracks rapidly increased. These phenomena indicated that the cyclic loading accelerated the damage process of polymer materials, and the extent of damage was also increased relative to the same level of monotonic loading.

Fig.11 presents the crack propagation data during cyclic loading and unloading. Here, plastic deformation was not very significant, and the crack location was distributed and dispersed during the initial loading. When the plastic deformation increased, some tensile cracks appeared around the original cracks. This verifies that the friction or extrusion on the surface of original cracks is one of the causes of new cracks.

5 Conclusions

a) A comparison between the experimental results and simulations show that the PFC^{2D} can describe the mechanical properties of the polymers. The primary meaning of this research lies in the fact that the PFC^{2D} numerical simulation can break through the limits of real lab tests. These limits are due to the equipment capacity and the experimental conditions. The model can predict some polymer responses under complex stress paths or complicated boundary conditions.

b) The polymer materials were characterized with triaxial cyclic loading-unloading tests under different confining pressures via PFC^{2D}. The results showed that the value of the elastic modulus decreased at first and then fluctuated within a narrow range. A greater confining pressure caused a larger modulus. The cumulative plastic strain increased slowly at first and then increased rapidly with axial strain. A greater confining pressure caused a smaller cumulative plastic strain. The confining pressure can improve the strength and resistance to the deformation of the polymer material.

c) The PFC^{2D} simulation results showed that at the same confining pressure, cyclic loading causes 9.65% more micro-cracks than monotonic loading. The damage rate obviously speeds up when the axial stress

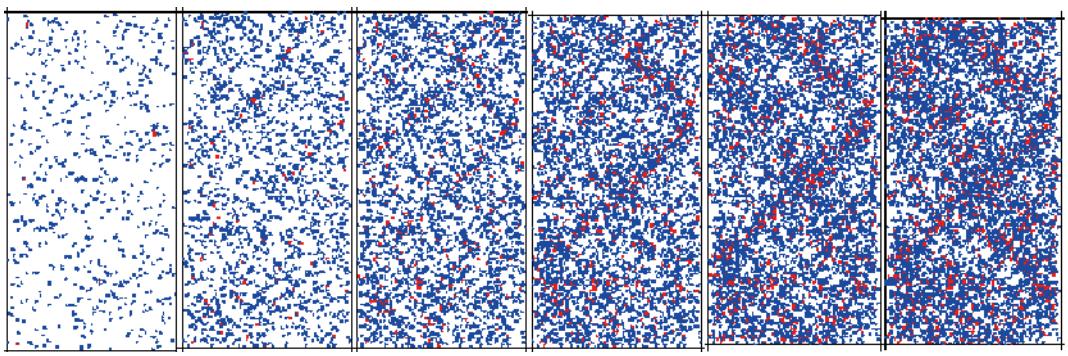

Fig.11 Micro-cracks in the specimen under cyclic loading at different plastic strains (σ_3=4 MPa; the plastic strains are 0.21%, 0.62%, 1.02%, 1.63%, 2.53%, and 3.5%)

is 40% of the peak stress. The number of micro-cracks becomes 'non-memory' under cyclic loading. The PFC^{2D} method can be used to quantitatively evaluate the damage behavior of polymer materials and estimate the fatigue life of materials under fatigue load.

d) Reference 6 shows that the mechanical properties of the polymers varied as its density changed. In this paper, the micro-parameters corresponding to the polymer had a density close to 0.35 g/cm^3 (about 0.3-0.4 g/cm^3). Other polymers with different densities would require a recalibration of the micro-parameters before the PFC^{2D} numerical experiments are carried out.

References

[1] SHI MS, WANG M, Luo J. Compressive Strength of Polymer Grouting Material at Different Temperatures[J]. *Journal of Wuhan University of Technology-Materials Science Edition*, 2010, 25(6): 962-965

[2] Uretek USA Inc. The URETEK Advantage for Public and Private Infrastructures[R]. *A URETEK USA White Paper*, 2005

[3] Barron B. Kansas DOT Decides to Go with Polyurethane to Correct 50 Miles of Highway 50[J]. *Roads & Bridges*, 2004, 12: 24-26

[4] WANG FM ,WANG JW, SHI MS. *et al*. *Directional Fracture Grouting with Polymer for Seepage Control for Dykes and Dams*[P]. China Patent 200910066334.8. 2009-11-2

[5] SHI MS, XIA WY, WAMG FM. *et al*. Experimental Study on Bond Performance Between Polymer Anchorage Body and Silt[J]. *Chinese Journal of Geotechnical Engineering*, 2014, 36 (4): 724-730

[6] SHI M S. *Research on Polymer Grouting Material Properties and Directional Fracturing Grouting Mechanism for Dykes and Dams*[D]. Dalian: Dalian University of Technology, 2011

[7] LIN YL, LU FY. Experimental Study of the Compressible Behavior of Low-Density Polyurethane Foam[J].*Chinese Journal of High Stress Physics*, 2006,20(1): 88-92

[8] LU ZX, GAO ZhT. Theoretical Prediction of Modulus and Yield Strength of High Density Foam Plastics[J]. *Science China Technological Sciences*, 1997, 27(4): 318-324

[9] Spence M, James AN, Lynch M et all. A Comparative Analysis of Techniques Used to Estimate the Mean Recoil Compressive Strength of High Performance Polymers[J]. *High Performance Polymers*, 2004, 16 (3): 381-390

[10] ZHANG JL, LU ZX. Finite Element Analysis for the Elastic Properties of Closed-cell Foams Based on a Tetrakaidecahedron Model[J]. *Journal of Mechanical Strength*, 2007, 29 (2): 315-319

[11] Lu ZX, Huang JX, Chen X. Analysis and Simulation of High Strain Compression of Anisotropic Open-Cell Elastic Foams[J]. *Science China Technological Sciences*, 2010, 53: 863-869

[12] Cundall PA. *PFC2D User's Manual*[Z]. Minnesota: Itasca Consulting Group Inc, 2004

[13] Potyondy DO, Cundall PA. A Bonded-particle Model For Rock[J]. *International Journal of Rock Mechanics and Mining Sciences*, 2004, 41 (8): 1329-1364

[14] Cho N, Martin CD, Sego DC. A Clumped Particle Model For Rock[J]. *Mechanics and Mining Sciences*, 2007, 44: 997-1 010

[15] XU JM, XIE Zh L, JIA HT. Simulation of Mesomechanical Rroperties of Limestone Using Particle Flow Code[J]. *Rock and soil mechanics*, 2010, 31 (p2): 390-395

[16] YANG SQ, PENG X, Ranjith PG, *et al*. Evaluation of Creep Mechanical Behavior of Deep-Buried Marble Under Triaxial Cyclic Loading. *Arabian Journal of Geosciences*, 2015, 8: 6 567-6 582

[17] LIAO XH, ZHOU J. Simulation of Plane Strain Test of Clay by Means of Particle Flow Code[J]. *Journal of Hydraulic Engineering*, 2002, 12: 11-17

[18] MARTIN CD, CHANDLER NA. The Progressive Fracture of Lacdu Bonnet Granite[J]. *International Journal of Rock Mechanics and Mining Sciences and Geomechanics Abstracts*,1994,31(6): 643-659

[19] ZHAO XG, LI PF. Damage and Dilation Characteristics of Deep Granite at Beishan Under Cyclic Loading-Unloading Conditions[J]. *Chinese Journal of Rock mechanics and Engineering*, 2014, 33 (9): 1 740-1 748